Printed in the Republic of Korea
ANALYTICAL SCIENCE & TECHNOLOGY
Vol. 38 No. 4, 238-249, 2025
https://doi.org/10.5806/AST.2025.38.4.238

Development of in-situ hydrogen permeation measurement technology based on volumetric analysis of polymer specimen under high pressure hydrogen environment

Ji Hun Lee★

Department of Measurement Science, University of Science and Technology, Deajeon 34113, South Korea
(Received March 17, 2025; Revised July 3, 2025; Accepted August 1, 2025)

Abstract: An in-situ high-pressure permeation measurement system was developed to evaluate the hydrogen permeation characteristics of polymer sealing materials in high-pressure hydrogen environments. This system enables real-time hydrogen permeation measurements following high-pressure hydrogen injection, utilizing a volumetric analysis method for accurate mole quantification of hydrogen gas. The system is equipped with a self-developed diffusion-permeation analysis program, facilitating precise evaluation of diffusivity, permeability, and solubility for hydrogen. To validate the system, hydrogen permeation tests were conducted on EPDM polymer containing carbon black filler, commonly used in O-ring for gas seals in high-pressure hydrogen infrastructure. The tests, performed at pressures ranging from 1 MPa to 10 MPa, revealed a decrease in hydrogen permeability and diffusivity with increasing pressure, while solubility remained unchanged. This indicates that the hydrogen permeation behavior in the polymer is predominantly influenced by diffusion rather than solubility. The hydrogen uptake data for the EPDM specimen conformed to Henry's law, with a high squared correlation coefficient of R^2 = 0.98. The system's reliability was further confirmed through uncertainty analysis, with all results within a permeability uncertainty of 9.1 %.

Key words: hydrogen permeation, diffusivity, volumetric analysis, in-situ, diffusion-permeation analysis program

1. Introduction

Hydrogen is a next-generation clean energy source with high energy density and zero carbon emissions, making it a key component in fuel cells, hydrogen storage, transportation and various industrial applications.[1-8] However, its small molecular size and high diffusivity allow it to permeate through many materials, leading to potential leakage and explosive risks during storage and transport.[9,10] Hydrogen permeation through metals and polymers can degrade their mechanical properties, causing hydrogen embrittlement in metals and structural changes in polymers, which may compromise long-term safety. Therefore, ensuring the reliability and safety of hydrogen infrastructure requires precise measurement and evaluation of hydrogen permeability across different materials.[11-20]

★ Corresponding author
Phone : +82-(0)10-4249-5507
E-mail : ljh93@kriss.re.kr

Hydrogen permeability measurement is crucial for assessing the performance and durability of materials used in hydrogen-related technologies. In hydrogen storage and transportation systems, O-ring materials with high hydrogen barrier properties are essential for high-pressure tanks, pipelines, and valves to minimize leakage risks.[21-30]

Accurate permeability measurements help in selecting and optimizing materials that ensure efficient and safe hydrogen containment.[31-35] In fuel cells and hydrogen energy systems, evaluating the hydrogen permeability of proton exchange membranes (PEMs) is critical for improving power generation efficiency, while analyzing the permeability of storage and supply systems in fuel cell vehicles (FCEVs) enhances their durability and operational safety.

Given the increasing demand for hydrogen as an energy carrier, the development of advanced hydrogen barrier materials has gained significant attention. Research efforts focus on improving the performance of polymer membranes, metal-polymer composites, and hydrogen-resistant coatings to mitigate hydrogen embrittlement and enhance long-term material stability.[36-39] Standardized permeability measurement techniques play a key role in evaluating and commercializing these materials for industrial applications.

Several methods are currently used to measure hydrogen and other gas permeability, including the differential pressure method, gas chromatography (GC), electrochemical methods, and gravimetric analysis. The differential pressure method[40-43] is widely used due to its simplicity and applicability to various materials, but it has limitations in detecting extremely low permeation rates. Gas chromatography (GC)[44-51] offers high precision by quantifying the concentration of permeated hydrogen, yet it is complex, time-consuming and costly.

The electrochemical method[51-55] enables high-sensitivity, real-time analysis but is limited to conductive materials and requires frequent calibration. The gravimetric method,[56-63] which measures weight changes due to hydrogen absorption and desorption, is relatively simple but lacks the precision needed for detecting small permeation rates. These limitations highlight the need for a more precise, reliable, and versatile measurement technique applicable across different materials and environmental conditions. In addition, optical spectroscopy, catalytic combustion and semiconductor-based gas sensors are their characteristic.[64-71]

This study aims to address the challenges associated with hydrogen permeation measurement by introducing a novel image-based volumetric analysis technique, integrated with the differential pressure method and a specialized diffusion-permeation analysis program.[72-75] By compensating for temperature and pressure fluctuations, this approach minimizes associated uncertainties, thereby improving both measurement accuracy and reliability. We investigate the hydrogen diffusivity, permeability, and solubility of ethylene propylene diene monomer (EPDM) polymers under pressures ranging from 1 MPa to 10 MPa, validating the effectiveness of the proposed technique through uncertainty evaluation. By enhancing the precision and reliability of hydrogen permeation parameter measurements, this study contributes to the development of safer and more efficient sealing materials, such as O-ring for hydrogen infrastructure, including H_2 transfer pipelines.

2. Specimen Preparation and Chemical Composition with Basic Property

EPDM (Ethylene Propylene Diene Monomer) exhibits excellent chemical resistance, low-temperature properties, and maintains stable elasticity over a wide temperature range of -40 to 150 °C, making it suitable for various applications.[76] Notably, when fillers such as silica or carbon black are added, the durability and barrier properties of EPDM under high-pressure hydrogen environments are enhanced.[77] Furthermore, high-hardness rubber materials are known to provide excellent resistance to degradation. To fabricate a high-hardness rubber specimen that can be used reliably at hydrogen high pressure, we selected EPDM containing a substantial amount of carbon black filler as the test material. The EPDM composite was supplied by Pyung Hwa Oil Seal

Industrial Co., Ltd. (Daegu, Korea). The EPDM matrix used in this study was Nodel® IP 4760P (Dow Chemical Company, Midland, TX, USA), containing 65 wt% ethylene and 5.0 wt% ethylidene norbornene (ENB). The carbon black (CB) was SRF CB (N774) manufactured by Orion Engineered Carbons, with an average particle size of 65 nm and a specific surface area of 32 m^2/g. The chemical composition and basic property of the fabricated material are presented in *Table* 1. The permeability experiments were conducted using disk-shaped specimens with an effective diameter of 35 mm and thickness of 2.2 mm.

Table 1. Chemical compositions and basic properties of carbon black-filled EPDM polymer

Chemical Compositions		EPDM composite
Polymer	EPDM	100 phr
Filler	carbon black (N774)	90 phr
Cure agent	Peroxide	5 phr
Basic properties	Density (g/cm^3)	1.192
	Hardness (Shore A)	90
	Tensile strength (MPa)	22.56

phr: parts per hundred rubber

3. Principle for Measuring Hydrogen Diffusivity, Permeability and Solubility

3.1. Measurement of hydrogen moles permeated by volumetric analysis

The molar amount of hydrogen gas permeated from the polymer after high-pressure hydrogen injection is measured in real time by utilizing the permeation cell and the volumetric gas collection method[77-79] in graduated cylinder, as shown in *Fig.* 1, with the change in the water level being analyzed through an image brightness analysis program. As the hydrogen gas is diffused and permeated across the specimen, it displaces the water inside the cylinder, causing the water level on the *Fig.* 1(b) to gradually decrease, forming a crescent-shaped meniscus (denoted as h). According to the manometer principle, the pressure inside the empty space of the cylinder, $P(t)$, as a function of time after pressure injection, can be expressed as the difference between the atmospheric pressure and the hydrostatic pressure, $\rho gh(t)$.[80-82]

$$P(t) = P_o(t) - \rho gh(t) \quad (1)$$

Here, $P(t)$ represents the atmospheric pressure in

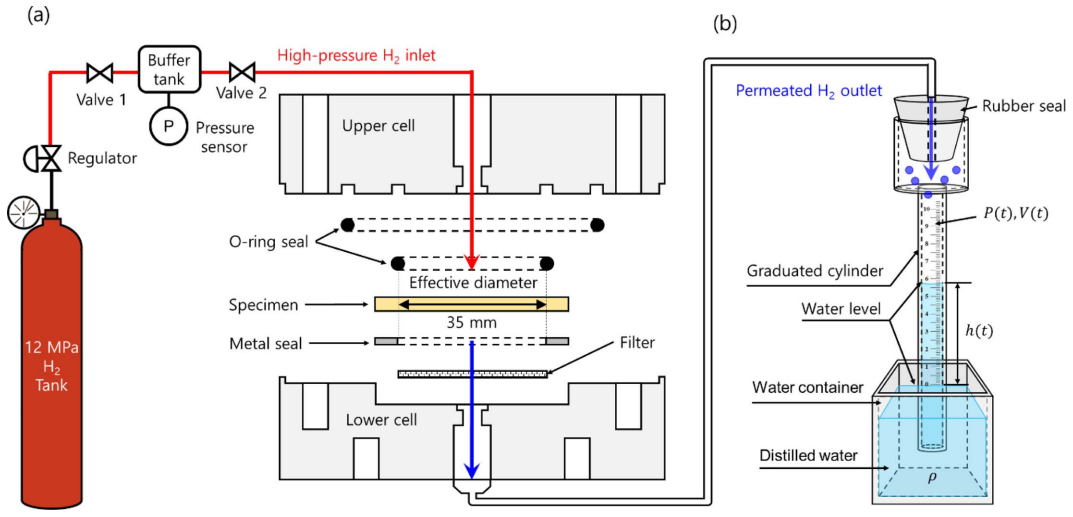

Fig. 1. Overall schematic representation of the in-situ high-pressure hydrogen permeation measuring system, (a) Diagram illustrating the high-pressure hydrogen injection process with the high pressure H_2 tank and permeation cell, (b) Volumetric measurement setup utilized for the precise quantification of permeated hydrogen. The red line illustrates the flow path of injected high-pressure hydrogen, while the blue line is the released pathway of the permeated hydrogen for H_2 molar amount measurement using cylinder. The blue area in (b) is the distilled water.

cylinder, ρ is the density of water at room temperature, g is the gravitational acceleration, and $h(t)$ is the measured water level inside the cylinder, taken from the surface of the water container as a function of time. By measuring $h(t)$, the volume of hydrogen gas (ΔV) permeated from the sample in the permeation cell can be determined. Using the ideal gas law ($PV = nRT$), the number of moles of hydrogen gas permeated (Δn) can then be calculated as follows.[81,82]

$$\Delta n\ [mol] = P(t)\Delta V(t)/RT(t) = [P_o(t) - \rho g h(t)]\Delta V(t)/RT(t),\ \Delta V(t) = Ah(t) \quad (2)$$

Here, R is the gas constant (8.20544×10^{-5} m³·atm/(mol·K)), $T(t)$ is the temperature inside the cylinder as a function of time, and A is the inner cross-sectional area of the cylinder. The molar quantity of hydrogen gas permeated, based on the change in water level due to the hydrogen permeated from the sample, is obtained from Eq. (2).

3.2. Overall system for measuring hydrogen diffusivity, permeability and solubility

Fig. 1 shows the developed in-situ H_2 permeation measuring system, which allows for water level measurements caused by hydrogen permeated from specimen. This system consists of high pressure hydrogen tank, permeation cell, graduated cylinder, one temperature sensor (UA10, DEKIST Co., Ltd., Yongin, Korea), one pressure sensor (UA52, DEKIST Co., Ltd.), a digital camera (D800, Nikon Co., Tokyo, Japan) and a computer running the developed program. The temperature and pressure obtained from the USB-based temperature and pressure sensors were used to calculate the hydrogen mole penetrated from the sample using Eqs. (1) and (2).

The high-pressure hydrogen injection process using the system in *Fig.* 1 is as follows.

First, Valve 2 is closed and Valve 1 is opened to pressurize hydrogen up to 10 MPa, considering the maximum storage pressure of the hydrogen tank (12 MPa), and store it in the buffer tank. Next, Valve 1 is closed and Valve 2 is opened, allowing hydrogen to be injected into the permeation cell up to the target pressure within a few second. The measurement begins by recording the time from the moment when Valve 2 is opened ($t = 0$). The quantitative measurement of permeated hydrogen was conducted using the volumetric measurement with cylinder shown in *Fig.* 1(b). The partially submerged cylinders, filled with distilled water, were used to measure the changes in water level caused by the hydrogen permeated from the sample.

3.3. Development of H_2 diffusion-permeation analysis program

Using the permeation measuring system in *Fig.* 1, the permeated hydrogen molar amount from the specimen were measured. The number of moles of the diffusing gas per unit area (A), $Q(t)$, can be expressed as follows[83]:

$$Q(t) = n(t)/A = lC_1 \times [Dt/l^2 - l/6 - 2/\pi^2 \sum_1^\infty (-1)^n/n^2 \exp(-Dn^2\pi^2 t/l^2)] \quad (3)$$

C_1 is the concentration at $x = 0$ in the high-pressure region. Here, x represents the spatial coordinate along the thickness of the specimen, where $x = 0$ corresponds to the high-pressure surface and $x = l$ to the low-pressure (permeate) surface. D is diffusivity. According to the experimental setup in the permeation cell, for a specimen with thickness l, the polymer specimen initially had zero concentration and the concentration at the face ($x = l$) through which the gas diffused was effectively maintained at zero concentration. Thus, we have finally obtained the Eq. (3).

The infinite series expansion in Eq. (3) was computed by summing the first 50 terms, as higher-order terms were negligible, with values smaller than 10^{-5}.[28,84] To ensure accuracy, we developed a specialized diffusion-permeation analysis program to include these 50 terms and calculate the diffusion coefficient using Eq. (3). This method proved to be more precise than the time lag (L) method, which is based on a simplified equation at infinite time, $L = l^2/6D$.[83]

The permeability was derived from the linear slope ($\Delta n/\Delta t$) representing the change in moles of hydrogen over time as follows:

$$P = (\Delta n/\Delta t)l/A\Delta P \quad (4)$$

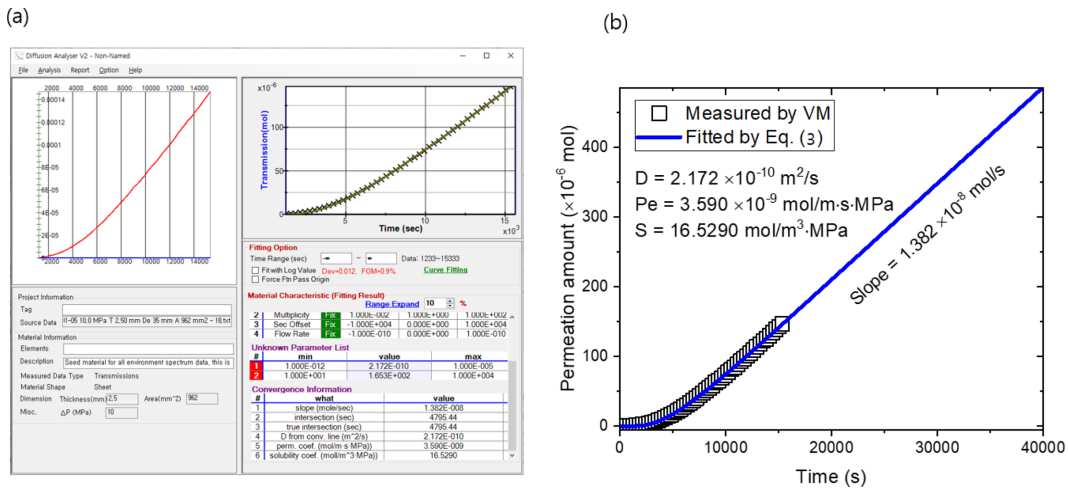

Fig. 2. (a) A diffusion-permeation analysis program for determining H_2 diffusivity, permeability and solubility using Eqs. (3) – (5) in EPDM polymer under injection pressure of 10 MPa, (b) replotted result showing diffusivity (*D*), peameability (*Pe*) and solubility (*S*), obtained by diffusion-permeation analysis program.

Here, A denotes the hydrogen contact area of the specimen, and ΔP is the pressure difference between the feed and permeate sides in the permeation cell. l is the specimen thickness. The hydrogen permeability was then determined from the steady-state flow rate using Eq. (4). Meanwhile, the H_2 solubility (S) is obtained from the diffusivity (D) and permeability (P) as follows[32,36]:

$$S = P/D \tag{5}$$

Fig. 2(a) shows an example of analyzing the hydrogen diffusion coefficient (D) and permeability (P) of an EPDM polymer using a self-developed hydrogen diffusion-permeability analysis program, based on molar amount of hydrogen measured at a hydrogen injection pressure of 10.0 MPa. The molar amount of hydrogen permeated at each time is obtained from Eq. (2). The analysis process is as follows:

First, after entering the thickness, effective permeation area (Area), experimental pressure difference (ΔP) and H_2 measured molar amount data for the disk-shaped specimen in the lower-left section, the curve fitting function, located in the middle-right section, is executed. As a result, the lower-right section displays the diffusivity, permeability and solubility values calculated using Eqs. (3) – (5), yielding $D = 2.172 \times 10^{-10}$ m²/s, $P_e = 3.590 \times 10^{-9}$ mol/m·s·MPa and $S = 16.529$ mol/m³·MPa, respectively. Utilizing this dedicated analysis program significantly reduces measurement time and provides additional information, such as the Figure of Merit (FOM) = 0.9 %, which indicates the deviation between equations and the measured data, as shown in the middle section of *Fig.* 2. The *Fig.* 2(b) is replotted results with permeation parameters obtained by diffusion-permeation analysis program. The blue line is the fitted result based on Eq. (3) by analysis program.

4. Measured Results and Discussions

4.1. Hydrogen permeation parameter versus injection pressure

Using a self-developed high-pressure hydrogen permeation system, the hydrogen permeation properties of EPDM polymer containing carbon black filler, designed for high-pressure hydrogen environments, were evaluated under various pressure conditions ranging from 1 MPa to 10 MPa. *Fig.* 3 presents the analysis of pressure dependence on permeation rate, permeability, diffusivity and solubility.

In *Fig.* 3(a), the hydrogen permeation rate exhibited an increasing trend with rising pressure. However,

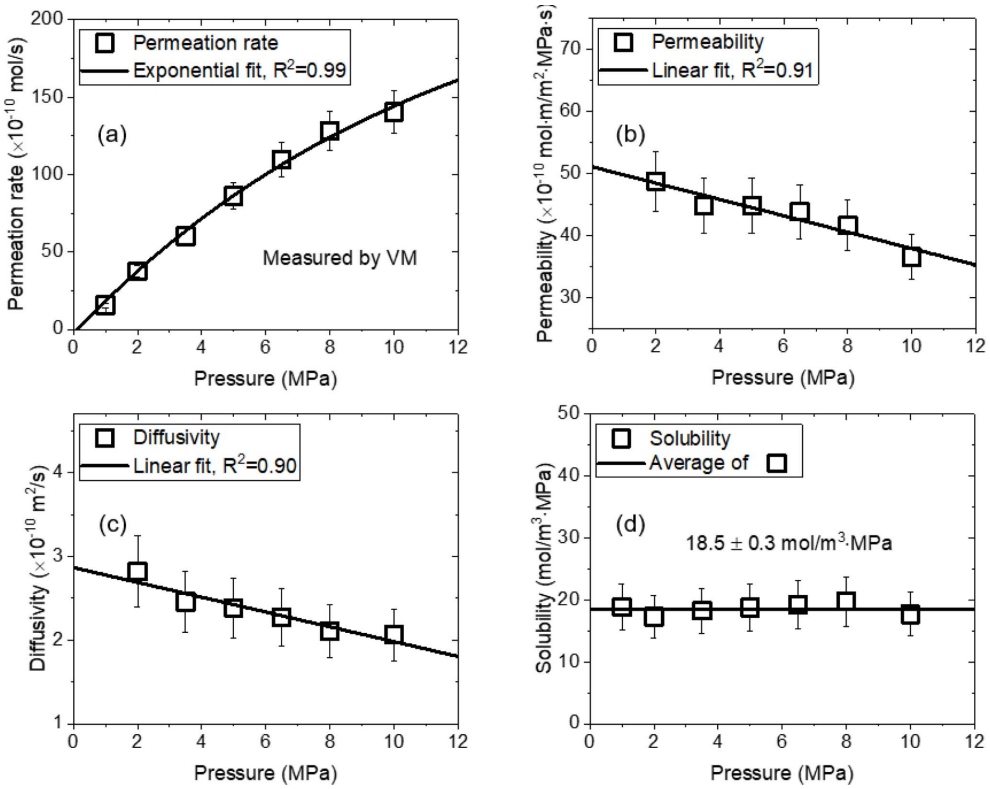

Fig. 3. High-pressure hydrogen (a) Permeation rate, (b) permeability, (c) diffusivity and (d) solubility versus pressure in carbon black-filled EPDM polymer.

the rate of increase gradually diminished at higher pressures. Theoretically, if permeability remains constant regardless of pressure, Eq. (4) suggests that the permeation rate should form a linear relationship passing through the origin. However, the observed decline in the rate of increase indicates that permeability decreases as pressure rises, as shown in *Fig.* 3(b). This behavior aligns with previous studies on the pressure dependence of gas permeability in polymers. According to Stern *et al.*[85] and Naito *et al.*[86] gas permeation in polymers can be classified into two categories based on the correlation between permeability and pressure. Condensable vapors, such as CO_2, N_2O, and organic vapors, exhibit a positive slope where permeability increases with pressure. In contrast, permanent gases with extremely low liquefaction temperatures, such as N_2 and He, show a negative slope, indicating a decrease in permeability with increasing pressure. Since hydrogen is also classified as a permanent gas, our results in *Fig.* 3(b) confirm a similar trend, where permeability decreases as pressure increases.

Fig. 3(c) illustrates the pressure dependence of diffusivity, which also decreases with increasing pressure. Gas diffusion in polymers follows the free volume model, where gas molecules migrate through transient free spaces generated by the thermal motion of polymer chains.[87,88] Fujiwara *et al.*[22] reported that, under high-pressure conditions, the available free volume within the polymer is reduced, limiting molecular diffusion and consequently lowering diffusivity.

In contrast, *Fig.* 3(d) shows that solubility remains relatively constant within the margin of uncertainty, regardless of pressure. This suggests that the decrease in permeability with increasing pressures is primarily attributed to reduced diffusivity due to the decrease in free volume, rather than changes in solubility.

Additionally, the permeation behavior of hydrogen in polymeric materials under high-pressure conditions is influenced not only by the simple dissolution-diffusion mechanism but also by complex factors such as internal pore structures, pressure-induced structural changes, and interactions between the polymer matrix and fillers.[89]

4.2. Hydrogen uptake versus injection pressure

Using the measured solubility values, the hydrogen uptake can be calculated by applying the following equation[32]:

$$\text{Hydrogen Uptake } [wtppm] = S \cdot m_{H2} \cdot P/d_s \quad (6)$$

where m_{H2} is the molecular weight of hydrogen gas (2.016 g/mol), P is the experimental pressure and d_s [g/m³] is the density of the specimen. The H_2 uptake was calculated using Eq. (6) for all solubility values presented in *Fig.* 3(d) and the results are shown in *Fig.* 4.

The behavior of hydrogen dissolved in polymeric materials can be generally interpreted using Henry's law or the Langmuir adsorption model. Henry's law describes the proportional increase in gas uptake with pressure, which is applicable when hydrogen is uniformly absorbed within the rubber matrix.[90] Meanwhile, the Langmuir adsorption model explains the phenomenon where hydrogen adsorbed onto the rubber matrix or filler surfaces reaches saturation at a certain pressure, preventing further adsorption.[91] As shown in *Fig.* 4, the hydrogen uptake results for EPDM polymer containing carbon black filler followed Henry's law with a squared correlation coefficient of $R^2 = 0.98$, indicating a quite good fit.

4.3. Uncertainty analysis

We have estimated the expanded relative uncertainty by finding the individual uncertainty factors. The uncertainty analysis was usually found in other literatures.[92-94] *Table* 2 presents the individual uncertainty factors and expanded uncertainties for H_2 permeability in our work. The primary sources of uncertainty in the permeability measurements were the repeated measurements and variations in the permeation area exposed to H_2 and in the sample thickness. The type A uncertainty for repeated permeability measurements was calculated based on five measurements. All type B uncertainties were determined using a rectangular distribution, dividing the uncertainty by $\sqrt{3}$.

The accuracy of the graduated cylinder is 0.5 %, and applying a rectangular distribution, the type B uncertainty is calculated as 0.3 %. For a 10 mL graduated cylinder with a minimum scale division of 0.1 mL, the corresponding uncertainty is 1 %. Since the resolution is half of this minimum value, applying a triangular distribution of dividing factor ($\sqrt{6}$), the

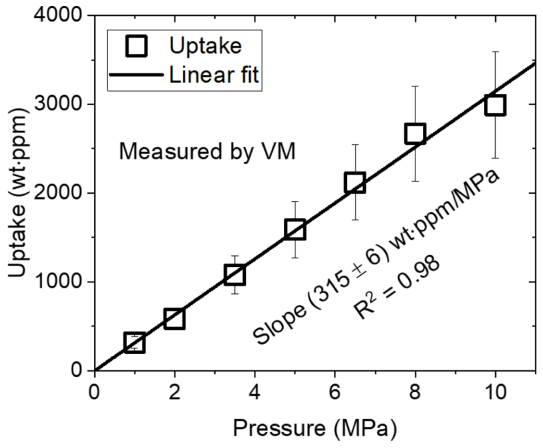

Fig. 4. H_2 uptake versus pressure in carbon black-filled EPDM polymer, calculated using Eq. (6).

Table 2. Individual uncertainty and expanded uncertainties for volumetric based differential pressure method system used in measuring the H_2 permeability

Individual uncertainty	Relative value (%)
– Repeated measurements	2.5
– Accuracy of the graduated cylinder	0.3
– Resolution of the graduated cylinder	0.2
– Volume of the permeated side in permeation cell	1.0
– Variation in the permeation area contacting with H_2	2.9
– Standard deviation between the data and Eq. (3)	0.9
– Thickness measurement of the sample	0.8
– Variation in the sample thickness	1.2
Combined standard uncertainty, u_c	4.3
Coverage factor, k	2.1
Expanded uncertainty, $U = ku_c$	9.1

type B uncertainty is determined to be 0.2 %. The uncertainty in the measured volume of the permeated side of the permeation cell was determined to be 1.0 %, derived from the standard deviation of the data.

Regarding the permeation area, the designed area of the permeation cell was 962 mm^2, but the O-ring seal caused a maximum area change of 48 mm^2. This led to a variation in the permeation area of up to 5 %, with a corresponding type B uncertainty of 2.9 %, calculated from the rectangular distribution. The standard deviation between the measured data and the fitting results using Eq. (3) was within 0.9 %, and this value was used to determine the type B uncertainty. The uncertainty in sample thickness measurements was 0.8 %, based on the calibration certificate, accuracy and resolution of the Vernier caliper. After mounting the sample between the holders, the maximum change in thickness was 2 %, leading to a type B uncertainty of 1.2 % for the change in thickness, considering the rectangular distribution by dividing factor $\sqrt{3}$.

The combined standard uncertainty was obtained as the root sum of squares of individual uncertainty, assuming the individual uncertainty was independent of one another. To obtain the relative expanded uncertainty, the combined standard uncertainty was multiplied by a coverage factor of 2.1 at 95 % confidence level, under the assumption of a normal distribution. The resulting expanded uncertainty for the H_2 permeability was 9.1 % as detailed in *Table* 2.

5. Conclusion

This study developed an in-situ hydrogen permeability measuring system to evaluate the hydrogen permeability characteristics of polymer sealing materials under high-pressure hydrogen environments, up to 10 MPa. The system was designed to measure the molar amount of hydrogen permeated over time after injecting high-pressure hydrogen, allowing for quantitative measurement using a volumetric analysis method. Additionally, a proprietary diffusion-permeation analysis program was employed to precisely assess key permeability characteristics, such as permeability, diffusivity and solubility.

Using this incorporate system, the high-pressure hydrogen permeability characteristics of EPDM polymer with carbon black filler were evaluated across a pressure range of 1 MPa to 10 MPa. The results showed that as pressure increased, permeability and diffusivity decreased, while solubility remained constant regardless of pressure. These findings suggest that hydrogen permeation behavior in polymer is significantly influenced by diffusion limitations due to a reduction in free volume, with the decrease in diffusivity being the primary factor responsible for the reduced permeability, rather than changes in solubility. It is also found that the hydrogen uptake results for EPDM polymer containing carbon black filler followed Henry's law with a quite a good squared correlation coefficient.

In conclusion, the experimental system and specialized analysis methods developed in this study provide a useful tool for quantitatively evaluating the sealing performance of polymer materials under high-pressure hydrogen conditions. This approach could play a crucial role in the future development of sealing materials like O-ring for high-pressure hydrogen applications. However, further research is needed to reduce uncertainties caused by Type A uncertainty and measurement stability, which would enable more precise analysis of hydrogen permeability characteristics.

References

1. H. Xie, Q. Yu, H. Lu, Y. Zhang, J. Zhang, and Q. Qin, *Int. J. Hydrog. Energy*, **42**(48), 28718-28731 (2017). https://doi.org/10.1016/j.ijhydene.2017.09.155
2. R. M. Dell, In 'Electrochemistry in Research and Development', 73-93, R. Kalvoda and R. Parsons, Eds., Springer, Boston, MA, 1985. https://doi.org/10.1007/978-1-4684-5098-9_11
3. J. K. Jung, I. G. Kim, K. S. Chung, and U. B. Baek, *Mater. Chem. Phys.*, **267**, 124653 (2021). https://doi.org/10.1016/j.matchemphys.2021.124653
4. Z. Wang, Z. Li, T. Jiang, X. Xu, and C. Wang, *ACS Appl. Mater. Interfaces*, **5**(6), 2013-2021 (2013). https://doi.org/10.1021/am3028553

5. J. K. Jung and J. H. Lee, *Sci. Rep.*, **14**(1), 1967 (2024). https://doi.org/10.1038/s41598-024-52168-3
6. C. Ma and A. Wang, *Opt. Lett.*, **35**(12), 2043-2045 (2010). https://doi.org/10.1364/OL.35.002043
7. M. A. Haija, A. I. Ayesh, S. Ahmed, and M. S. Katsiotis, *Appl. Surf. Sci.*, **369**, 443-447 (2016). https://doi.org/10.1016/j.apsusc.2016.02.103
8. Z. Li, Z. Yao, A. A. Haidry, T. Plecenik, L. Xie, L. Sun, and Q. Fatima, *Int. J. Hydrog. Energy*, **43**(45), 21114-21132 (2018). https://doi.org/10.1016/j.ijhydene.2018.09.051
9. N. Liu, M. L. Tang, M. Hentschel, H. Giessen, and A. P. Alivisatos, *Nat. Mater.*, **10**(8), 631-636 (2011). https://doi.org/10.1038/nmat3029
10. Z. Wang, Y. Hu, W. Wang, X. Zhang, B. Wang, H. Tian, Y. Wang, J. Guan, and H. Gu, *Int. J. Hydrog. Energy*, **37**(5), 4526-4532 (2012). https://doi.org/10.1016/j.ijhydene.2011.12.004
11. H. M. Kang, M. C. Choi, J. H. Lee, Y. M. Yun, J. S. Jang, N. K. Chung, S. K. Jeon, J. K. Jung, J. H. Lee, J. H. Lee, Y. W. Chang, and J. W. Bae, *Polymers*, **14**(6), 1151 (2022). https://doi.org/10.3390/polym14061151
12. J. K. Jung, I. G. Kim, and K. T. Kim, Curr. *Appl. Phys*., **21**, 43-49 (2021). https://doi.org/10.1016/j.cap.2020.10.003
13. J. K. Jung, I. G. Kim, K. T. Kim, U. B. Baek, and S. H. Nahm, *Curr. Appl. Phys*., **26**, 9-15 (2021). https://doi.org/10.1016/j.cap.2021.03.005
14. H. Kang, J. Bae, J. Lee, Y. Yun, S. Jeon, N. Chung, J. Jung, U. Baek, J. Lee, Y. Kim, and M. Choi, *Polymers*, **16**(8), 1065 (2024). https://doi.org/10.3390/polym16081065
15. J. K. Jung, K. T. Kim, N. K. Chung, U. B. Baek, and S. H. Nahm, *Polymers*, **14**(7), 1468 (2022). https://doi.org/10.3390/polym14071468
16. S. Nishimura, *Int. Polym. Sci. Technol.*, **41**(6), 27-34 (2014). https://doi.org/10.2324/gomu.86.360
17. J. Yamabe and S. Nishimura, In 'Gaseous Hydrogen Embrittlement of Materials in Energy Technologies', 769-816, R. P. Gangloff, and B. P. Somerday, Eds., Woodhead Publishing, Sawston, UK, 2012. https://doi.org/10.1533/9780857093899.3.769
18. N. Aibada, R. Manickam, K. K. Gupta, and P. Raichurkar, *Int. J. Text. Eng. Process.*, **3**(1), 12-18 (2017).
19. R. R. Barth, K. L. Simmons, and C. W. S. Marchi, 'Polymers for Hydrogen Infrastructure and Vehicle Fuel Systems: Applications, Properties, and Gap Analysis. SAND2013-8904', Sandia National Laboratories, Livermore, CA, 2013.
20. M. Honselaar, G. Pasaoglu, and A. Martens, *Int. J. Hydrog. Energy*, **43**(27), 12278-12294 (2018). https://doi.org/10.1016/j.ijhydene.2018.04.111
21. Y. Wang, Y. Pang, H. Xu, A. Martinez, and K. S. Chen, *Energy Environ. Sci*., **15**(6), 2288-2328 (2022). https://doi.org/10.1039/D2EE00790H
22. H. Fujiwara, H. Ono, K. Onoue, and S. Nishimura, *Int. J. Hydrog. Energy*, **45**(53), 29082-29094 (2020). https://doi.org/10.1016/j.ijhydene.2020.07.215
23. J. K. Jung, Y. I. Moon, K. S. Chung, and K. T. Kim, *Macromol. Res.*, **28**(6), 596-604 (2020). https://doi.org/10.1007/s13233-020-8080-6
24. I. Profatilova, F. Fouda-Onana, M. Heitzmann, T. Bacquart, A. Morris, J. Warren, F. Haloua, and P. A. Jacques, *Int. J. Hydrog. Energy*, **65**, 837-843 (2024). https://doi.org/10.1016/j.ijhydene.2024.04.055
25. N. C. Menon, A. M. Kruizenga, K. J. Alvine, C. S. Marchi, A. Nissen, and K. Brooks, Proceedings of the ASME 2016 Pressure Vessels and Piping Conference. Volume 6B: Materials and Fabrication, American Society of Mechanical Engineers, Vancouver, BC, PVP2016-63713, V06BT06A037 (2016). https://doi.org/10.1115/PVP2016-63713
26. Y. I. Moon, J. K. Jung, G. H. Kim, and K. S. Chung, *Phys. B Condens. Matter*, **608**, 412870 (2021). https://doi.org/10.1016/j.physb.2021.412870
27. S. U. Zhanguo, W. Zhang, A. Abdulwahab, S. Saleem, Y. Yao, A. Deifalla, and M. Taghavi, *Process Saf. Environ. Prot.*, **173**, 317-331 (2023). https://doi.org/10.1016/j.psep.2023.03.015
28. J. K. Jung, J. H. Lee, S. K. Jeon, U. B. Baek, S. H. Lee, C. H. Lee, and W. J. Moon, *Polymers*, **15**(1), 162 (2023). https://doi.org/10.3390/polym15010162
29. J. K. Jung, U. B. Baek, S. H. Lee, M. C. Choi, and J. W. Bae, *J. Polym. Sci.*, **61**(6), 460-471 (2023). https://doi.org/10.1002/pol.20220494
30. B. L. Choi, J. K. Jung, U. B. Baek, and B. H. Choi, *Polymers*, **14**(5), 861 (2022). https://doi.org/10.3390/polym14050861
31. C. H. Lee, J. K. Jung, S. K. Jeon, K. S. Ryu, and U. B. Baek, *J. Magn.*, **22**(3), 478-482 (2017). https://doi.org/10.4283/JMAG.2017.22.3.478

32. J. H. Lee, Y. W. Kim, and J. K. Jung, *Polymers*, **15**(19), 4019 (2023). https://doi.org/10.3390/polym15194019
33. J. H. Lee, Y. W. Kim, D. J. Kim, N. K. Chung, and J. K. Jung, *Polymers*, **16**(2), 280 (2024). https://doi.org/10.3390/polym16020280
34. J. H. Lee, Y. W. Kim, N. K. Chung, H. M. Kang, W. J. Moon, M. C. Choi, and J. K. Jung, *Polymer*, **311**, 127552 (2024). https://doi.org/10.1016/j.polymer.2024.127552
35. C. H. Lee, J. K. Jung, K. S. Kim, and C. J. Kim, *Sci. Rep.*, **14**(1), 5319 (2024). https://doi.org/10.1038/s41598-024-55101-w
36. J. K. Jung, J. H. Lee, J. S. Jang, N. K. Chung, C. Y. Park, U. B. Baek, and S. H. Nahm, *Sci. Rep.*, **12**(1), 3328 (2022). https://doi.org/10.1038/s41598-022-07321-1
37. Y. Moon, H. Lee, J. Jung, and H. Han, *Sci. Rep.*, **13**(1), 7846 (2023). https://doi.org/10.1038/s41598-023-34565-2
38. G. H. Kim, Y. I. Moon, J. K. Jung, M. C. Choi, and J. W. Bae, *Polymers*, **14**(1), 155 (2022). https://doi.org/10.3390/polym14010155
39. J. K. Jung, C. H. Lee, U. B. Baek, M. C. Choi, and J. W. Bae, *Polymers*, **14**(3), 592 (2022). https://doi.org/10.3390/polym14030592
40. M. Wang, J. Liu, Y. Bai, D. Zheng, and L. Fang, *Energy*, **288**, 129852 (2024). https://doi.org/10.1016/j.energy.2023.129852
41. X. Shi, C. Tan, and F. Dong, *IEEE Trans. Instrum. Meas.*, **73**, 7508515 (2024). https://doi.org/10.1109/TIM.2024.3470252
42. Q. Yang, N. Jin, Y. Deng, and D. Wang, *IEEE Sens. J.*, **21**(2), 2149-2158 (2021). https://doi.org/10.1109/JSEN.2020.3019602
43. Y. R. Deng, N. D. Jin, Q. Y. Yang, and D. Y. Wang, *Sensors*, **19**(12), 2723 (2019). https://doi.org/10.3390/s19122723
44. J. K. Jung, I. G. Kim, K. S. Chung, Y. I. Kim, and D. H. Kim, *Sci. Rep*., **11**(1), 17092 (2021). https://doi.org/10.1038/s41598-021-96266-y
45. J. K. Jung, I. G. Kim, K. S. Chung, and U. B. Baek, *Sci. Rep*., **11**(1), 4859 (2021). https://doi.org/10.1038/s41598-021-83692-1
46. J. K. Jung, K. T. Kim, and K. S. Chung, *Mater. Chem. Phys*., **276**, 125364 (2022). https://doi.org/10.1016/j.matchemphys.2021.125364
47. R. Slater, K. Tharmaratnam, S. Belnour, M. K. H. Auth, R. Muhammed, C. Spray, D. Wang, B. De Lacy Costello, M. García-Fiñana, S. Allen, and C. Probert, *Sensors*, **24**(15), 5079 (2024). https://doi.org/10.3390/s24155079
48. J. K. Jung, I. G. Kim, K. T. Kim, K. S. Ryu, and K. S. Chung, *Polym. Test*., **93**, 107016 (2021). https://doi.org/10.1016/j.polymertesting.2020.107016
49. F. Hardoyono and K. Windhani, *Flavour Fragr. J*., **38**(6), 451-463 (2023). https://doi.org/10.1002/ffj.3759
50. Z. Huang, W. Yang, Y. Zhang, J. Yin, X. Sun, J. Sun, G. Ren, S. Tian, P. Wang, and H. Wan, *Anal. Chem*., **96**(45), 17960-17968 (2024). https://doi.org/10.1021/acs.analchem.4c02561
51. A. Hinojo, E. Lujan, J. Abella, and S. Colominas, *Fusion Eng. Des*., **204**, 114483 (2024). https://doi.org/10.1016/j.fusengdes.2024.114483
52. W. M. Seleka, K. E. Ramohlola, K. D. Modibane, and E. Makhado, *Int. J. Hydrog. Energy*, **68**, 940-954 (2024). https://doi.org/10.1016/j.ijhydene.2024.04.240
53. C. Wang, J. Yang, J. Li, C. Luo, X. Xu, and F. Qian, *Int. J. Hydrog. Energy*, **48**(80), 31377-31391 (2023). https://doi.org/10.1016/j.ijhydene.2023.04.167
54. T. Cowen, S. Grammatikos, and M. Cheffena, *Analyst*, **149**(8), 2428-2435 (2024). https://doi.org/10.1039/D4AN00045E
55. E. Gorbova, G. Balkourani, C. Molochas, D. Sidiropoulos, A. Brouzgou, A. Demin, and P. Tsiakaras, *Catalysts*, **12**(12), 1647 (2022). https://doi.org/10.3390/catal12121647
56. R. Kendler, F. Dreisbach, R. Seif, S. Pollak, and M. Petermann, Thermochim, *Acta*, **664**, 128-135 (2018). https://doi.org/10.1016/j.tca.2018.05.001
57. W. Schabel, P. Scharfer, M. Kind, and I. Mamaliga, *Chem. Eng. Sci.*, **62**(8), 2254-2266 (2007). https://doi.org/10.1016/j.ces.2006.12.062
58. J. K. Jung, I. G. Kim, S. K. Jeon, and K. S. Chung, *Rubber Chem. Technol.*, **94**(4), 688-703 (2021). https://doi.org/10.5254/rct.21.79880
59. X. Zhu, W. Ahmed, K. Schmidt, R. Barroso, S. J. Fowler, and C. F. Blanford, *IEEE Trans. Instrum. Meas.*, **73**, 9520508 (2024). https://doi.org/10.1109/TIM.2024.3485428
60. L. Quercia, I. Khomenko, R. Capuano, M. Tonezzer, R. Paolesse, E. Martinelli, A. Catini, F. Biasioli, and C. Di Natale, *Sens. Actuators B Chem.*, **347**, 130580 (2021). https://doi.org/10.1016/j.snb.2021.130580
61) Y. R. Shaltaeva, B. I. Podlepetsky, and V. S. Pershenkov,

Eur. J. Mass Spectrom., **23**(4), 217-224 (2017). https://doi.org/10.1177/1469066717720 79
62. J. A. Imonigie, R. N. Walters, and M. M. Gribb, *Instrum. Sci. Technol.*, **34**(6), 677-695 (2006). https://doi.org/10.1080/10739140600964010
63. C. Pérès, F. Begnaud, and J. L. Berdagué, *Anal. Chem.*, **74**(10), 2279-2283 (2002). https://doi.org/10.1021/ac0111558
64. R. Xie, S. Guan, and Z. Tan, *Opt. Commun.*, **574**, 131105 (2025). https://doi.org/10.1016/j.optcom.2024.131105
65. M. Basso, V. Paolucci, V. Ricci, E. Colusso, M. Cattelan, E. Napolitani, C. Cantalini, and A. Martucci, *ACS Appl. Mater. Interfaces*, **16**(42), 57558-57570 (2024). https://doi.org/10.1021/acsami.4c13003
66. X. Zhang, B. Ojha, H. Bichlmaier, I. Hartmann, and H. Kohler, *Sensors*, **23**(10), 4679 (2023). https://doi.org/10.3390/s23104679
67. D. Del Orbe Henriquez, I. Cho, H. Yang, J. Choi, M. Kang, K. S. Chang, C. B. Jeong, S. W. Han, and I. Park, *ACS Appl. Nano Mater.*, **4**(1), 7-12 (2020). https://doi.org/10.1021/acsanm.0c02794
68. S. Tamura and N. Imanaka, *Bunseki Kagaku*, **70**(6), 327-334 (2021). https://doi.org/10.2116/bunsekikagaku.70.327
69. A. Alaghmandfard, S. Fardindoost, A. L. Frencken, and M. Hoorfar, *Ceram. Int.*, **50**(17), 29026-29043 (2024). https://doi.org/10.1016/j.ceramint.2024.05.259
70. S. K. Kwon, J. N. Kim, H. G. Byun, and H. J. Kim, *Electrochem. Commun.*, **169**, 107834 (2024). https://doi.org/10.1016/j.elecom.2024.107834
71. Y. Li, Z. Yuan, H. Ji, F. Meng, and H. Wang, *IEEE Trans. Ind. Electron.*, **71**(9), 11661-11670 (2024). https://doi.org/10.1109/TIE.2023.3329254
72. J. H. Lee and J. K. Jung, *Sensors*, **24**(23), 7699 (2024). https://doi.org/10.3390/s24237699
73. J. K. Jung, I. G. Kim, S. K. Jeon, K. T. Kim, U. B. Baek, and S. H. Nahm, *Polym. Test.*, **99**, 107147 (2021). https://doi.org/10.1016/j.polymertesting.2021.107147
74. J. K. Jung, J. H. Lee, S. K. Jeon, N. H. Tak, N. K. Chung, U. B. Baek, S. H. Lee, C. H. Lee, M. C. Choi, H. M. Kang, J. W. Bae, and W. J. Moon, *Int. J. Mol. Sci.*, **24**(3), 2865 (2023). https://doi.org/10.3390/ijms24032865
75. J. K. Jung, K. T. Kim, and U. B. Baek, *Curr. Appl. Phys.*, **37**, 19-26 (2022). https://doi.org/10.1016/j.cap.2022.02.005
76. R. Karpeles and A. Grossi, In 'Handbook of Elastomers', 863-894, A. K. Bhowmick and H. L. Stephens, Eds., CRC Press, Boca Raton, FL, 2000. https://doi.org/10.1201/9781482270365
77. J. K. Jung, *Polymers*, **16**(5), 723 (2024). https://doi.org/10.3390/polym16050723
78. J. K. Jung, K. T. Kim, U. B. Baek, and S. H. Nahm, *Polymers*, **14**(4), 756 (2022). https://doi.org/10.3390/polym14040756
79. J. K. Jung, S. K. Jeon, K. T. Kim, C. H. Lee, U. B. Baek, and K. S. Chung, *Sci. Rep.*, **9**(1), 13035 (2019). https://doi.org/10.1038/s41598-019-49692-y
80. J. K. Jung, Y. I. Moon, and K. S. Chung, *J. Korean Phys. Soc.*, **76**(5), 416-425 (2020). https://doi.org/10.3938/jkps.76.416
81. J. K. Jung, J. H. Lee, Y. W. Kim, and N. K. Chung, *Sens. Actuators B Chem.*, **418**, 136240 (2024). https://doi.org/10.1016/j.snb.2024.136240
82. J. K. Jung, C. H. Lee, M. S. Son, J. H. Lee, U. B. Baek, K. S. Chung, M. C. Choi, and J. W. Bae, *Polymers*, **14**(4), 700 (2022). https://doi.org/10.3390/polym14040700
83. J. Crank, 'The Mathematics of Diffusion', Clarendon Press, Oxford, UK, 1979.
84. J. K. Jung, J. H. Lee, J. Y. Park, and S. K. Jeon, *Polymers*, **16**(15), 2158 (2024). https://doi.org/10.3390/polym16152158
85. S. A. Stern, S. M. Fang, and R. M. Jobbins, *Journal of Macromolecular Science, Part B: Physics*, **5**, 41-69 (1971). https://doi.org/10.1080/00222347108212520
86. Y. Naito, D. Bourbon, K. Terada, and Y. Kamiya, *J. Polym. Sci. B Polym. Phys.*, **31**(6), 693-697 (1993). https://doi.org/10.1002/polb.1993.090310609
87. G. Choudalakis and A. D. Gotsis, *Curr. Opin. Colloid Interface Sci.*, **17**(3), 132-140 (2012). https://doi.org/10.1016/j.cocis.2012.01.004
88. C. H. Lee, S. H. Park, J. K. Jung, K. S. Ryu, S. H. Nahm, J. Kim, and Y. Chen, *Solid State Commun*., **134**(6), 419-423 (2005). https://doi.org/10.1016/j.ssc.2005.01.052
89. M. Sadrzadeh, M. Amirilargani, K. Shahidi, and T. Mohammadi, *J. Membr. Sci.*, **342**(1-2), 236-250 (2009). https://doi.org/10.1016/j.memsci.2009.06.047
90. R. Sander, *Atmos. Chem. Phys*., **15**(8), 4399-4981 (2015). https://doi.org/10.5194/acp-23-10901-2023.
91. D. D. Do, H. D. Do, and K. N. Tran, *Langmuir*, **19**(14), 5656-5668 (2003). https://doi.org/10.1021/la020191e

92. J. K. Jung, A. Faisal, Y. S. Lee, and K. T. Kim, *Meas. Sci. Technol*., **26**(9), 095004 (2015). https://doi.org/10.1088/0957-0233/26/9/095004
93. J. K. Jung, A. Faisal, Y. S. Lee, and K. T. Kim, *IEEE Trans. Instrum. Meas.*, **64**(6), 1564-1569 (2015). https://doi.org/10.1109/TIM.2015.2416457
94. J. K. Jung, E. So, S. H. Lee, and D. Bennett, *IEEE Trans. Instrum. Meas*., **60**(7), 2634-2641 (2011). https://doi.org/10.1109/TIM.2011.2126190